A Numerical Investigation of X-Shaped Transverse Rib Roughened Solar Air Heater

Munna Kumar[1] O. P. Shukla[2] Manjit Kumar[3]
[1]PG Scholar [2,3]Assistant Professor
[1,2,3]Department of Mechanical Engineering
[1,2]CIST College Bhopal, India [3]SIRT College, India

Abstract— A numerical investigation has been performed to study the effects of different rib shapes on heat transfer and fluid flow characteristics through transversely roughened rectangular channels for Reynolds number ranging from 3800 to 15,000 and subjected to uniform heat flux of 1000 W/m2. Considering single-phase approach, the three-dimensional continuity, Navier-Stokes, and energy equations developed for the physical model have been solved by using the finite volume method (FVM). The optimization was carried out by using various Rib shapes (X-section rib channel & Square section rib channel) in in-line and different aspect ratios (Dh=33.33, Aspect ratio of duct W/H=5, Relative roughness pitch P/e=7.14, Relative roughness height e/D=0.042) to reach the optimal geometry of the rib with maximum Performance Evaluation Criterion (PEC). The highest PEC was obtained for the X-section rib at Re =3800 is 1.703. For the X-section rib channel, the increase in average Nusselt number value is about 162.48% more than the smooth channel and the use of the X-section rib channel compare with Square section rib channel shows a higher average Nusselt number around 17.70%.

Key words: Artificial Roughness, Solar Air Heater, Roughness Geometry, Nusselt Number, Friction Factor, Thermo Hydraulic Performance, Reynolds Number

I. INTRODUCTION

The Solar air heater is one of the basic equipment through which solar energy is converted into thermal energy. Solar air heater is a type of solar thermal system where air is heated in a collector and either transferred directly to the interior space or to a storage medium. A conventional solar air heater generally consists of an absorber plate, a rear plate, insulation below the rear plate, transparent cover on the exposed side, and the air flows between the absorbing plate and rear plate. The air gets heated up while the absorber plate absorbs the heat. The hot air is drawn through the plates with a blower which is operated electrically. The main applications of solar air heater are space heating, seasoning of timber, curing of industrial products and these can also be effectively used for curing/drying of concrete/clay building components. The other applications of solar air heater are drying of agro and allied products, food items such as fruits, vegetables, chilies, tea-leaves, fish, salt, etc. The solar air heater can be used in many industrial activities (drying/heating) such as chemical, pharmaceutical, limited areas of textiles and hosieries, tannery, edible oil, etc.

A. Techniques to Break the Laminar Sub-layer

Employing ribs or grooves on the inner surface of channels has been one of the frequent passive approaches to break the laminar sub-layer and create local wall turbulence due to flow separation and reattachment between successive corrugations, which reduces the thermal resistance and significantly enhances rate of heat transfer. The ribbed channel, because of its effectiveness in heat transfer, is a good candidate for engineering applications, such as cross-flow heat exchanger, gas turbine airfoil cooling design, solar air heater, blade-cooling system, and gas cooled nuclear reactor.

A lot of studies have been carried out in the literature on artificially roughened surfaces for heat transfer increase but most of the studies were reported with two opposite or all the four walls roughened for high Reynolds number range in the area of gas turbine airfoil cooling system, gas cooled nuclear reactors, cooling of electronic equipment, shipping machineries, combustion chamber liners, missiles, re-entry vehicles, ship hulls and piping networks etc. Several investigators have attempted to design an artificially roughened rectangular duct which can enhance the heat transfer with minimum pumping losses with two or four roughened surfaces. Artificial roughness in the form of fine wires of different shapes and in various arrangements has been used to create turbulence near the wall or to break the boundary layer. Various researchers have investigated the effects of rib shapes on the heat transfer and friction in a rectangular channel with roughened surfaces.

A.S. Yadav, J.L. Bhagoria [1] A numerical investigation on the heat transfer and fluid flow characteristics of fully developed turbulent flow in a rectangular duct having repeated transverse square sectioned rib roughness on the absorber plate has been carried out. The commercial finite-volume CFD code ANSYS FLUENT (ver. 12.1) is used to simulate turbulent airflow through artificially roughened solar air heater. The Naviere Stokes equations and the energy equation are solved in conjunction with a low Reynolds number RNG k-ε turbulence model. Twelve different configurations of square sectioned rib (P/E= 7.14 - 35.71 and e/D= 0.021 - 0.042) have been considered. The flow Reynolds number of the duct varied in the range of 3800 -18,000, most suitable for solar air heater. The effects of relative roughness pitch and relative roughness height on Nusselt number and friction factor have been discussed and the results are compared with the square sectioned rib roughened duct and smooth duct under similar flow conditions to investigate the enhancement in Nusselt number and friction factor. Roughness and flow parameters for artificially roughened solar air heater have been optimized by considering the thermo hydraulic performance parameter based on constant pumping power requirement. It has been found that the square sectioned transverse rib roughened duct with P/e=10.71 and e/D=0.042 offers the best thermo-hydraulic performance parameter for the investigated range of parameters. Wang and Sunder [2] experimentally examined the characteristics of the heat transfer and friction in a square duct roughened by transversely placed, various-shaped ribs. The shapes of the ribs were square, equilateral-triangular, trapezoidal with decreasing height in the flow

direction and trapezoidal with increasing height in the flow direction. It was shown that the trapezoidal-shaped rib with decreasing height has the highest heat transfer enhancement factor than any other rib shapes for same rib pitch (P) and rib height (e). Ahn [3] experimentally investigated the effect of rib shapes on the heat transfer and friction in a square duct. It was shown that the triangular-shaped rib has the highest heat transfer performance than any other rib profile for same rib pitch (P) and rib height (e).

Chandra et al. [4] experimentally investigated the effect of rib shapes on the heat transfer and friction in a square channel. It was shown that the square ribs produce higher heat transfer augmentation for same rib pitch (P) and rib height (e) than any other rib shapes.

Liou and Hwang [5] experimentally examined the fully developed turbulent flow in a rectangular duct roughened with three rib shapes, namely square, semicircular and triangular cross section. The results showed that the for same rib pitch (P) and rib height (e) highest thermal performance was obtained for the square-ribbed duct and lowest friction factor was obtained for the semicircular ribbed duct. But geometric and operating parameters relevant to solar air heater are different from the above mentioned applications. In the case of solar air heaters, roughness elements have to be considered only on one wall, which is the only heated wall comprising the absorber plate. These applications make the fluid flow and heat transfer characteristics distinctly different from those found in case of two roughened walls and four heated wall duct. In the case of solar air heaters, only one wall of the rectangular air passage is subjected to uniform heat flux while the remaining three walls are insulated. Literature also revealed that the practically most suitable range of Reynolds number for solar air heater lies between 3800 and 18,000

Kumar and Saini [6] performed a CFD analysis of fluid flow and heat transfer characteristics of a solar air heaters having arc shaped rib roughness on the absorber plate. The heat transfer and flow analysis of artificially roughened solar air heater were carried out using 3-D model. FLUENT 6.3.26 commercial CFD code was used as a solver. In order to find out the best turbulent model, authors tested four different turbulent models namely shear stress transport k-ω, standard k-ε , Renormalization group (RNG) k-ε and realizable k-ε for smooth solar air heater. Renormalization group (RNG) k-ε model was employed to simulate the fluid flow and heat transfer. The results of the simulation were successfully validated with experimental results. Overall enhancement ratio with a maximum value of 1.7 was obtained for the roughness geometry corresponding to relative arc angle (a/90) of 0.333 and relative roughness height (e/D) of 0.0426 by adopting CFD approach. Gupta et al. [7] suggested that the solar air heater systems operating in a specified range of Reynolds number (3800 -15,000) would show better thermo-hydraulic performance. Bilen and Yapici [8] studied the effect of orientation angle of the turbulence promoters located on the channel wall on the heat transfer. They showed that the highest heat transfer rate is achieved when the promoter orientation angle is 45 degrees. [9] Investigated the air turbulent forced convection heat transfer in a 2-D channel flow over periodic transverse grooves numerically. The grooves were on the lower channel wall subjected to a constant heat flux condition while the upper wall was insulated. The analysis showed that the groove-widths to channel-height ratio of Bill = 0,75 has thermal enhancement factor of about 1.33.

II. NOMENCLATURE

Ac	surface area of absorber plate (m2)
Cp	specific heat of air(J/kg/K)
D	equivalent or hydraulic diameter of duct(m)
E	rib height(m)
H	heat transfer coefficient(W/m2/K)
H	depth of duct(m)
I	turbulence intensity/intensity of solar radiation (W/m2)
K	thermal conductivity of air(W/m/K)
L	length of duct(m)
L_1	inlet length of duct(m)
L_2	test length of duct(m)
L_3	outlet length of duct(m) m mass flow rate(kg/s)
D_P	pressure drop(Pa)
P	pitch (m) q_u useful heat flux(W/m2)
Q_u	useful heat gain(W)
Q_L	heat loss from collector(W)
Q_t	heat loss from top of collector(W)
T_o	fluid outlet temperature(K)
T_i	fluid inlet temperature(K)
Ta	ambient temperature(K)
T_{pm}	mean plate temperature(K)
T_{am}	mean air temperature(K)
T_w	wall temperature(K)
Tm	bulk mean temperature(K)
U_L	overall heat loss coefficient(W/m2/K)
V	velocity of air in the duct(m/s)
W	width of duct(m)
Dimensionless parameters	
e/D	relative roughness height
F	friction factor
Nu	Nusselt number
Pr	Prandtl number
p/e	relative roughness pitch
R	roughness function
Re	Reynolds number
W/H	duct aspect ratio

Table 1:

III. CHANNEL GEOMETRY & BOUNDARY CONDITION

A. Physical Model

The three-dimensional solar air heater used in the simulations is a rectangular duct with periodically distributed roughness on its upper wall forming the fluid flow. A generic, schematic representation of the rectangular duct.3.1, test, and Fig.3.2 shows the details of the test section. The heat transfer was performed numerically using solar air heater with a rectangular duct height of H=20mm. The total length of solar air heater duct is L=640 mm. The length of test section is L_2= 280 mm, with an upstream (inlet section) L1= 245 mm to ensure a fully developed flow in the test section. The downstream section (exit section) has the length of L_3=115

mm which is used to prevent the occurrence of adverse pressure effects caused by reversed flow through the computational domain. In this study, the rib height and the rib width are e = 1.4 mm and w =1.4 mm, respectively. The dimensions for rectangular case are shown in Fig.3.3 In addition, the heat transfer enhancement is studied as a function of three families, which are represented, by the Reynolds numbers, type of fluid, and rib shapes. X-shapes of ribs as shown in Fig.3.4 have been investigated in the present work.

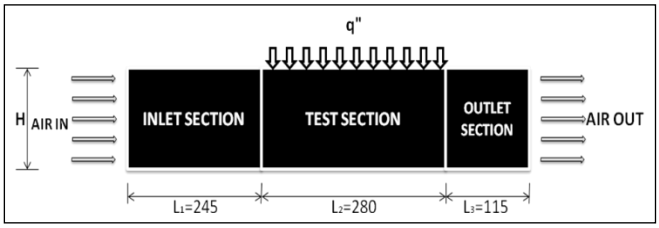

Fig. 3.1: Schematic Diagram of the Investigated Region of Smooth Rectangular Channel

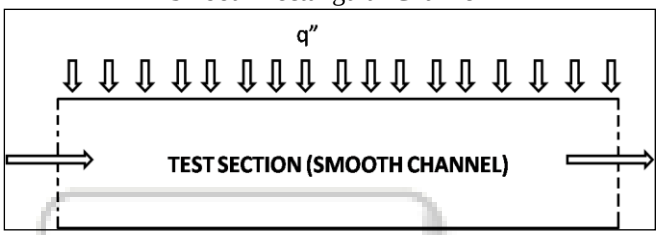

Fig. 3.2: Schematic Diagram of the Investigated Region of Smooth Rectangular Channel

1) Problem Formulation

The present work is concerned with carrying out three-dimensional simulations on an artificially roughened solar air heater, through which air flows. The air heater internal surface was roughened with the help of transverse-square and thin (high aspect ratio) ribs. The ribs were arranged in different patterns namely one wall only, staggered and in-line on upper face

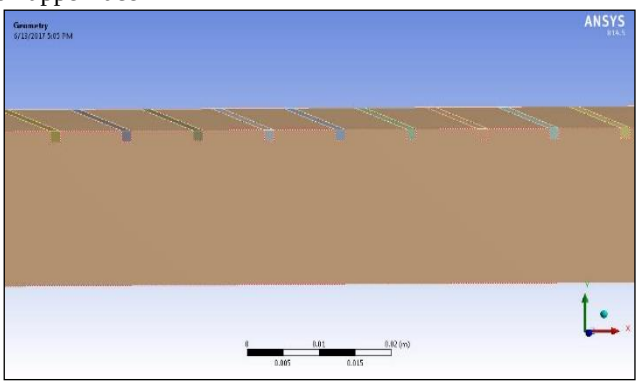

Fig. 3.3: Schematic Diagram of Rib Geometry (Rectangular Section)

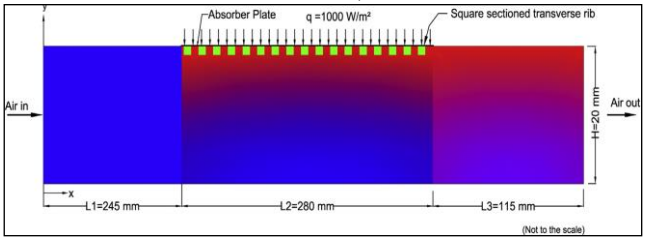

Fig. 3.3.1: Sketch of the Computational Domain of Rectangular Rib Section

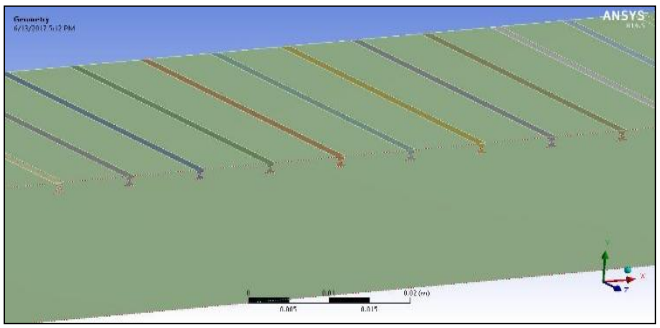

Fig. 3.4: Schematic Diagram of Rib Geometry (X-section)

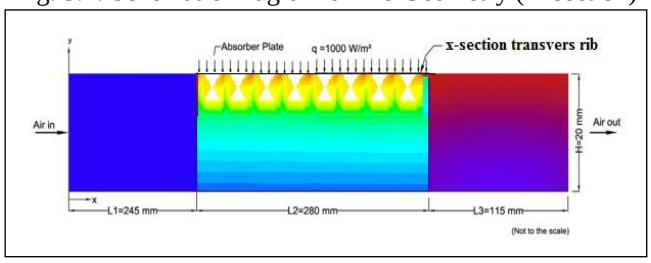

Fig. 3.4.1: Sketch of the Computational Domain of Rectangular Rib Section

IV. GOVERNING EQUATION

The steady 3-dimensional form of the continuity, the time-independent incompressible Naviere Stokes equations and the energy equation governs turbulent airflow through artificially roughened solar air heater. These equations can be written as follows:

The assumptions made on the operating conditions of the ribbed channel are as follows

1) The ribbed channel operates under steady-state conditions
2) The fluid is incompressible and remains in single-phase along the channel
3) The properties of the fluid and channel material are independent of temperature
4) Uniform heat flux is incident on upper wall

The single-phase governing equations for flow and heat transfer in the ribbed channel can be written in the Cartesian tensor system as

A. Continuity Equation

Law of Conservation of Mass: Fluid mass is always conserved. (Equation 1)

$$\frac{\partial(\rho u_i)}{\partial x_i}=0 \qquad (1)$$

Where ρ the density of fluid and ui is axial velocity

B. Momentum Equation

Newton's 2nd Law: The sum of the forces on a fluid particle is equal to the rate of change of momentum. (Equation 2)

$$\frac{\partial}{\partial x_i}(\rho u_i u_j) = -\frac{\partial p}{\partial x_i} + \frac{\partial}{\partial x_j}\left[\mu\left(\frac{\partial u_i}{\partial x_j}+\frac{\partial u_j}{\partial x_j}+\frac{\partial u_i}{\partial x_j}\right)\right] + \frac{\partial}{\partial x_j}\left(-\rho\overline{u_i u_j}\right) \quad (2)$$

Here μ is the viscosity of fluid,

Where μ, u_i and u_j are the fluid viscosity, fluctuated velocity, and the axial velocity, respectively, and the term the turbulent shear stress. The Reynolds-averaged approach to turbulence modeling requires that the Reynolds

stresses $-\rho\overline{u_i u_j}$, in Eq. (2) needs to be modelled. For closure of the equations, the k-ε turbulence model is chosen. A common method employs the Boussinesq hypothesis to relate the Reynolds stresses to the mean velocity gradients:

$$-\rho\overline{u_i u_j} = \mu_t\left(\frac{\partial u_i}{\partial x_j} + \frac{\partial u_j}{\partial x_j}\right) \quad (3)$$

C. Energy Equation

First Law of Thermodynamics: The rate of head added to a system plus the rate of work done on a fluid particle equals the total rate of change in energy. (Equation 3)

$$\frac{\partial}{\partial x_i}(\rho u_i T) = \frac{\partial}{\partial x_j}\left[(\Gamma + \Gamma_t)\frac{\partial T}{\partial x_j}\right] \quad (4)$$

Where Γ and Γ_t, are molecular thermal diffusivity and turbulent thermal diffusivity, respectively and are given by

$$\Gamma = \frac{\mu}{pr}, \text{ and } \Gamma_t = \frac{\mu}{pr_t} \quad (5)$$

The turbulent viscosity term μ_t is to be computed from an appropriate turbulence model. The expression for the turbulent viscosity is given as

$$\mu_t = \rho c_\mu \frac{k^2}{\varepsilon} \quad (6)$$

There are two additional equations for the k-ε turbulent model:

1) Turbulent kinetic energy (k)

$$\frac{\partial}{\partial x_i}(\rho k u_i) = \frac{\delta}{\delta x_j}\left[\left(\mu + \frac{\mu_t}{\sigma_k}\right)\frac{\partial k}{\partial x_j}\right] + G_{k-}\rho\varepsilon \quad (7)$$

2) Rate of dissipation (ε)

$$\frac{\partial}{\partial x_i}(\rho\varepsilon u_i) = \frac{\delta}{\delta x_j}\left[\left(\mu + \frac{\mu_t}{\sigma_\varepsilon}\right) + C_{1\varepsilon}\frac{\varepsilon}{k}G_k - C_{2\varepsilon}\rho\frac{\varepsilon^2}{k}\right] \quad (8)$$

In the above equation, G_k represents the rate of generation of the turbulent kinetic energy due to mean velocity gradients while ρε is its destruction rate. The σ_k and σ_ε are effective Prandtl numbers for turbulent kinetic energy and rate of dissipation, respectively; $C_{1\varepsilon}$ and $C_{2\varepsilon}$ are constants. G_k is written as:

$$G_k = -\rho u_i u_j \frac{\overline{\delta u_j}}{\delta x_j} \quad (9)$$

The boundary values for the turbulent quantities near the wall are specified with the enhanced wall treatment method. Cμ=0.09, $C_{1\varepsilon}$=1.44, $C_{2\varepsilon}$ =1.92, σ_k=1.0, σ_ε=1.3 and Pr_t=0.9 are chosen to be empirical constants in the turbulence transport equations.

The governing equations are solved using a finite volume approach and the SIMPLE algorithm. The solutions are considered to be converged when the normalized residual values reach 10^{-5} for all variables.

D. Parameters Involved

To analyze and compare the flow characteristics and heat transfer of different configurations of ribbed channels, following as

1) Hydraulic diameter (D_h):

$$D_h = \frac{4A}{P_h} \quad (10)$$

Where A is cross-sectional area and P_h is wetted perimeter of the cross-section

2) Reynolds number (Re):

$$Re = \frac{\rho u_m}{\mu} D_h \quad (11)$$

Where u_m mean velocity of fluid in cross-section here is Reynolds numbers are taken a range of 3800-15000 in order to have turbulent regime.

3) Nusselt number (Nu):

$$Nu = \frac{hD_h}{k} \quad (12)$$

Where h is convective heat transfer co-efficient and k is thermal conductivity of air

4) Friction factor for fully developed turbulent flow(f)

The friction factor is computed by pressure drop, P across the length of test section, and can be obtained by

$$f = \frac{2\Delta pD}{\rho Lu^2} \quad (13)$$

Where Δp is the pressure difference between inlet and outlet:

$$\Delta p = p_{av,\ inlet} - p_{av,\ outlet} \quad (14)$$

Here, $p_{av,inlet}$ and $p_{av,\ outlet}$ are the inlet and outlet average pressure, respectively.

5) Thermo-hydraulic performance parameter (THPP):

Under a constant pumping power, the thermo hydraulic performance parameter has been used to estimate how effectively an artificially roughened surface enhances the heat transfer under constant pumping power constraints. In order to analyze overall performance of a solar air heater, thermo-hydraulic performance should be evaluated by considering thermal and hydraulic characteristics of the solar air heater simultaneously. Webb and Eckert suggested a Thermo hydraulic performance parameter which is used to compare the heat transfer of artificially roughened duct to that of a smooth duct. A value of thermo hydraulic performance parameter greater than one ensures the effectiveness of using an enhancement device and can be used to compare the performance of number of arrangements to decide the best among these.

$$\text{Thermo hydraulic performance parameter} = \frac{Nu_r/Nu_s}{(f_r/f_s)^{1/3}} \quad (15)$$

Here Nu_s and f_s are the Nusselt number and friction factor for smooth channel, respectively and Nu_r and f_r are the Nusselt number and friction factor for rough surface with different ribs shape.

E. Selection of Appropriate Turbulence Model

Results were validated by comparing the obtained numerical data with the available correlations developed for a smooth channel and also with the numerically conducted studies on transversely roughened channels.

First, the Nusselt number and friction factor obtained from the present smooth channel for turbulent flow are compared with correlations of Dittus-Boelter and Blasius, respectively.

F. Correlations of Dittus-Boelter

$$Nu = 0.023Re^{0.8}pr^{0.4} \text{ (for heating)} \quad (16)$$

Correlations of Blasius:

$$f = 0.316Re^{-0.25} \text{ for } 3000 < Re < 20000 \quad (17)$$

The Nusselt number (Nu) of channel has been calculated by using three different turbulence models, including, the standard k-ε turbulence model, the renormalized group (RNG) k-ε turbulence model, and the standard k-ω turbulence model, and found that the RNG k-ε turbulence model gives the better result of Nusselt number as compared to other turbulence model when compared with the value of Nusselt number obtained from Dittus-Boelter equation.

V. VALIDATION OF NUMERICAL METHOD

A. Validation of Smooth Model

The present numerical results on heat transfer and friction characteristics in a smooth wall channel are first validated in terms of Nusselt number and friction factor. The Nusselt number and friction factor obtained from the present smooth channel are, respectively, compared with the correlations of Dittus-Boelter and Blasius correlation [01] for turbulent flow in duct.

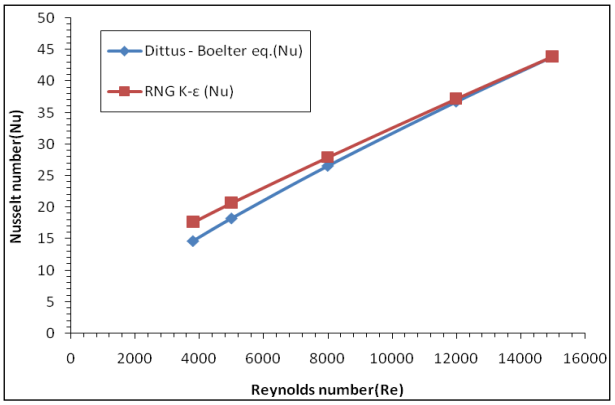

Fig 5.1.1 validation of Nusselt Number for Smooth Channel

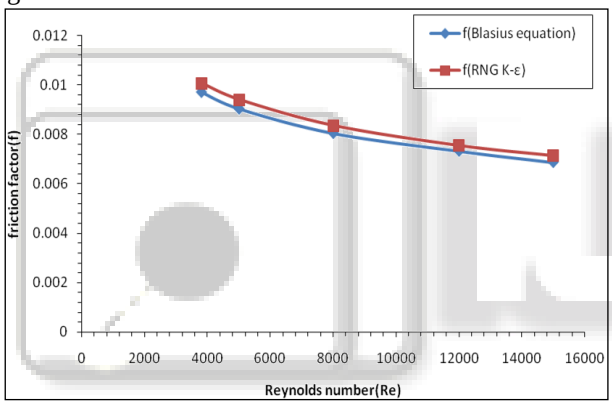

Fig. 5.1.2 validation of Friction Factor of Smooth Channel

Fig. 5.1.1 and Fig.5.1.2 show respectively, a comparison of Nusselt number and friction factor obtained from the present work with those from correlations of equation (16) and (17). In the figures, the present results reasonably agree well within ±10% for both friction factor correlation of Blasius and Nusselt number correlation of Dittus-Boelter.

B. Result & Discussion

The effects of different rib shapes fitted in inline, different rib aspect ratios, and Reynolds number on the thermal and flow fields are analyzed and discussed in this section. The present numerical results on heat and flow friction characteristics in a uniform heat flux channel equipped with 1.4 mm dimple height of two different rib shapes (square rib & X-section rib) are presented in the form of Nusselt number and friction factor.

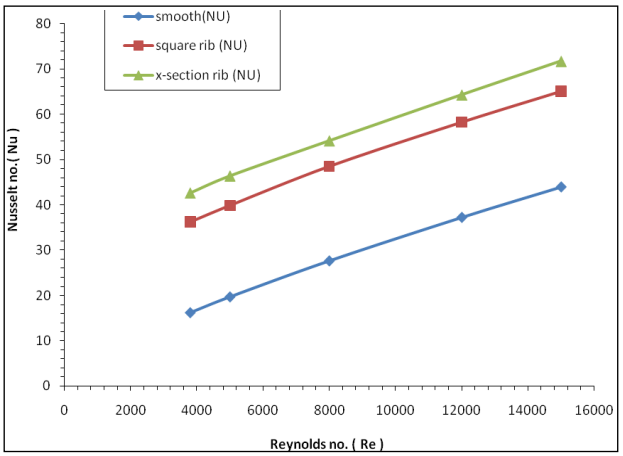

Fig. 5.2.1: Variation of Nu Number with Reynolds Number for Various Rib Shapes

The effect of different dimple shapes has been considered to examine their influence on the thermal and flow fields. The computed average Nusselt number distribution with Reynolds numbers for various rib shapes are presented in Fig.5.2.1. It can be seen that as the Reynolds number increases, the average Nusselt number also increases. The large Reynolds number is attributed to the higher velocity, which can lead to disturb the flow, and thus the heat transfer is increases. In all cases, the rib channel flows gave higher values of Nusselt number than that for smooth channel flow due to the induction of high re-circulation flow and thin boundary layer in the rib channels, leading to higher temperature gradients. It can be seen in Fig.5.2.1 the rib channel with X-section shape provides the highest average Nusselt number at all Reynolds numbers. Fig5.2.1 shows that all the X-section rib channel and Square section rib channel yields higher average Nusselt number than the smooth one for all Reynolds number values. For the X-section rib channel, the increase in average Nusselt number value is about 162.48% more than the smooth channel. The use of the X-section rib channel compare with Square section rib channel shows a higher average Nusselt number around 17.70%.

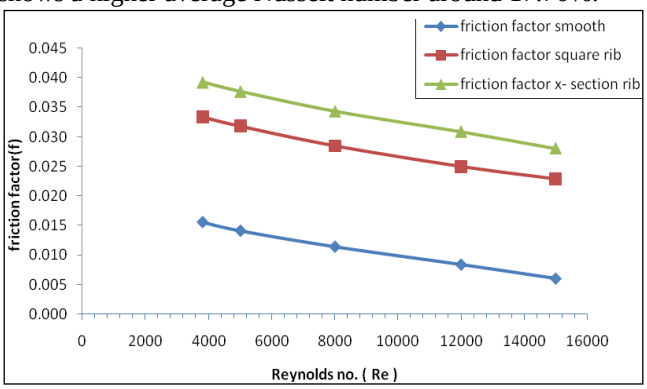

Fig. 5.2.2: Variation of Friction factor (f) with Reynolds Number for Various Rib Shapes

The effect of using the rib Turbulators on the isothermal pressure drop across the tested channel is presented in Fig.5.2.2. The variation of the pressure drop is shown in term of friction factor with Reynolds number. In the figure, it is apparent that the use of rib Turbulators leads to a substantial increase in friction factor over the smooth channel. The increases in friction factor for dimple

Turbulators is considerably higher than that for the smooth channel and is much higher than that in Nusselt number, however. This can be attributed to flow blockage, higher surface area and the act caused by the reverse flow. As expected, the friction factor obtained from the X-section rib & square rib channel is substantially higher than that from smooth one. The mean increase in friction factor of using the X-section rib & square rib channel one is in a range of 5 to 8 times over the smooth channel. The losses mainly come from the dissipation of the dynamical pressure of the air due to high viscous losses near the wall, to the extra forces exerted by reverse flow and to higher friction of increasing surface area and the blockage because of the presence of the ribs.

C. Performance Evaluation

The Nusselt number ratio, Nu_{rib}/Nu_s, defined as a ratio of average Nusselt number of rib channel to average Nusselt number of smooth channel and the value of ratio plotted against the Reynolds number value, is shown in Fig. 5.3.1. In this figure, the Nusselt number ratio tends to decrease with the rise of Reynolds number From 3,800 to 15,000 for all ribs shows a slightly increase for higher Reynolds number value. The average Nu_{rib}/Nu_s, values for the X-section rib & Square section rib are respectively, around, 2.717, and 2.401 at Re no. 3800.

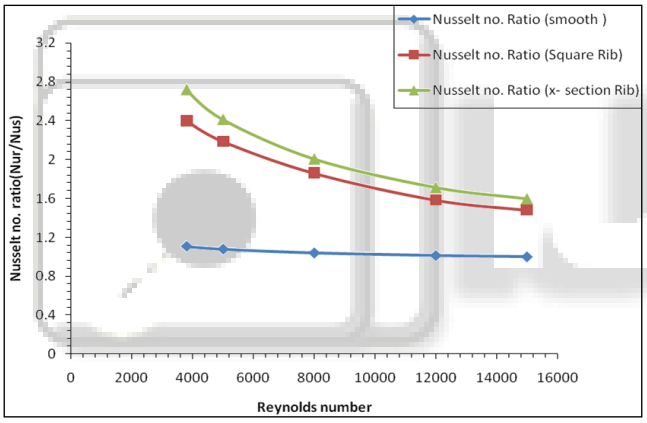

Fig. 5.3.1: Variation of Nusselt number ratio, Nu (rib)/Nu (smooth) with Reynolds number

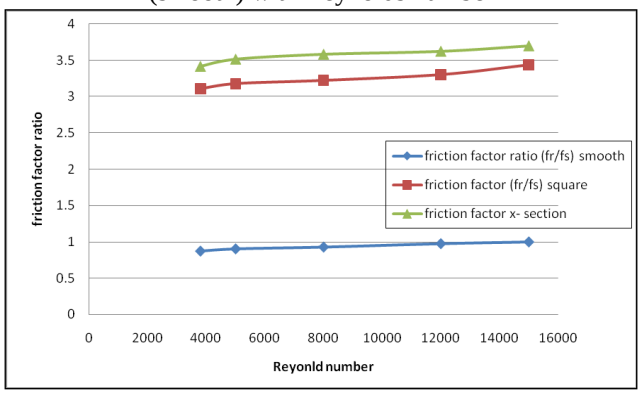

Fig. 5.3.2: Variation of friction factor ratio, f(rib)/f(smooth) with Reynolds number

The fr/fs values for the X-section rib channel & Square rib channel are respectively, around 3.4129 and 3.11 at Re=3800.

Fig.5.3.3 shows the variation of the Performance Evaluation Criteria (PEC) with Reynolds number for all rib shapes. For all, the data obtained by measured Nusselt number and friction factor values are compared at a similar pumping power. It is seen in the figure that the Performance Evaluation Criteria (PEC) is above unity for all shapes dimple channel when Reynolds number (Re) varies from 3800 to 15,000.

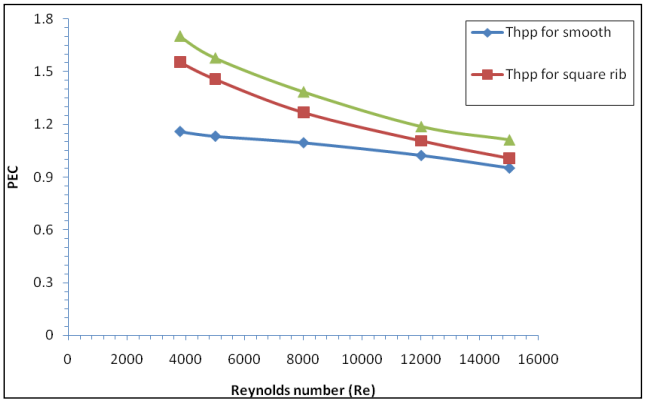

Fig. 5.3.3: Variation of Performance Evaluation Criteria (PEC) with Reynolds Number

Fig.5.3.3 shows that for each test channel, the values of PEC have quite similar trend in the considered range of Reynolds number. It is seen that the PECs for the channels decrease with increasing Reynolds number which means there is an optimum Reynolds number, corresponding to the maximum PEC for each type of geometry. The optimum Reynolds number is related to Re = 3800 for all geometries. The value of PEC index for X-section rib channel has been found to be the best among all rib shapes and is about 1.703 at the lowest value of Reynolds number. It also shows that the variation of PEC is high at low Reynolds number but at higher Reynolds number there is low variation in PEC.

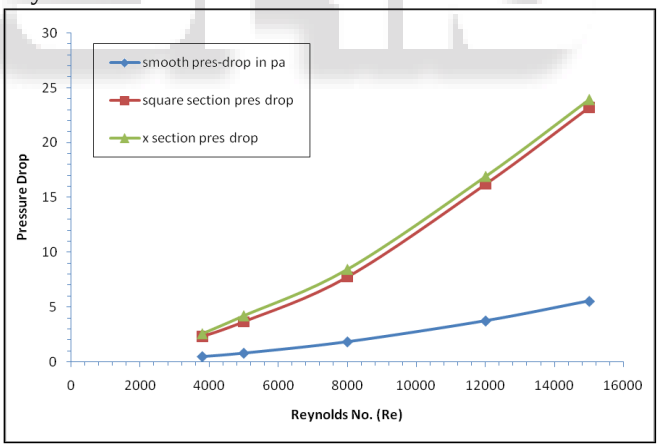

Fig. 5.3.4: Variation of Pressure Drop with Reynolds Number

Fig5.3.4 shows that all the X-section rib channel and Square section rib channel yields higher average Pressure drop than the smooth one for all Reynolds number values. The value of Pressure drop is increases with increases in Reynolds no for all geometry ribs and the higher value of Pressure drop is 23.936 at Re no 15000. For the X-section rib channel, the increase in average Pressure drop value is about 400% more than the smooth channel at Re=3800. The use of the X-section rib channel compare with Square section rib channel shows a higher average Pressure drop around 348.36% at Re=3800.

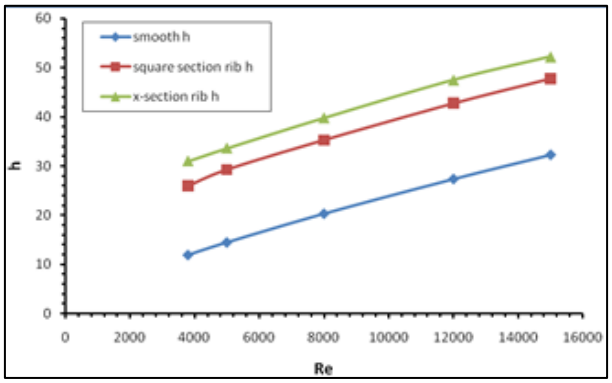

Fig. 5.3.5: Variation of Convection Heat Transfer Coefficient (h) with Reynolds No

Fig 5.3.5 shows that all the X-section rib channel and Square section rib channel yields higher Convection heat transfer coefficient (h) than the smooth one for all Reynolds number values. The value of Convection heat transfer coefficient (h) is increases with increases in Reynolds no for all geometry ribs and the higher value of Convection heat transfer coefficient (h) is 52.213 at Re no 15000. For the X-section rib channel, the increase in Convection heat transfer coefficient (h) value is about 160.38% more than the smooth channel at Re=3800. The use of the X-section rib channel compare with Square section rib channel shows a higher Convection heat transfer coefficient (h) around 19.20% at Re=3800.

VI. Conclusions & Scope for Future Work

A. Conclusions

In this work, a rectangular channel provided with transverse rib (X-section, Square Section) constant heat flux equal of 1000 W/m^2 has been carried out by means of FLUENT 14.5. The aim of the investigation consists into find out the optimal shape of rib at different Reynolds number, between 3800 and 15,000, in order to ensure maximum heat transfer rate and PEC.

B. According to the Results

1) Results found from Dittus-Boelter and Blasius equation respectively is compared [1] to validate the turbulence model used for CFD analysis and it is found that Renormalization Group (RNG) k-epsilon turbulence model results show good agreement with the Dittus-Boelter and Blasius empirical correlation results.
2) X-section rib channel shows the maximum average Nusselt number as compared to other rib shape channel for all value of Re from 3800 to 15,000, and its value is approximately 2.717 times more of smooth channel at Re=3,800.
3) X-section rib channel shows the maximum average friction factor as compared to other rib shape channel for Re vary from 3800 to 15,000, and its value 3.7 times more of smooth channel.
4) In X-section rib channel shows maximum value of Performance Evaluation Criteria (PEC) is 1.703, Square section rib channel of PEC is 1.596, all the value is found at Reynolds number Re=3,800.
5) X-section rib channel shows maximum value of Performance Evaluation Criteria (PEC) is 1.703, for all values of Re from 3800 to 15,000, i.e. X-section rib channel exhibits optimum PEC.
6) For the X-section rib channel, the increase in average Nusselt number value is about 162.48% more than the smooth channel. The use of the X-section rib channel compare with Square section rib channel shows a higher average Nusselt number around 17.70%.
7) For the X-section rib channel, the increase in average Pressure drop value is about 400% more than the smooth channel at Re=3800. The use of the X-section rib channel compare with Square section rib channel shows a higher average Pressure drop around 348.36% at Re=3800.
8) For the X-section rib channel, the increase in Convection heat transfer coefficient (h) value is about 160.38% more than the smooth channel at Re=3800. The use of the X-section rib channel compare with Square section rib channel shows a higher Convection heat transfer coefficient (h) around 19.20% at Re=3800.

1) Scope for Future Work

- Number of ribs can be varied in the rectangular channel to analyze numerically and study the effects on the thermal and fluid flow characteristics in turbulent flow.
- The transverse rib can be arranged in staggered form on both sides (top and bottom) of rectangular channel to analyze numerically and study the effects of different rib shapes (X-section, Square section), on the thermal and fluid flow characteristics in turbulent flow.
- Different type of working fluid can be used in the rib shape channel to find the best thermo-hydraulic performance for a given fluid.

References

[1] A.S. Yadav, J.L. Bhagoria, A numerical investigation of square sectioned transverse rib roughened solar air heaterInt. International Journal of Thermal Sciences 79 (2014) 111-131.
[2] L. Wang, B. Sunden, Experimental investigation of local heat transfer in a square duct with various-shaped ribs, Heat Mass Transf. 43 (2007) 759 - 766.
[3] S.W. Ahn, The effect of roughness type on friction factors and heat transfer in roughened rectangular duct, Int. Commun. Heat Mass Transf. 28 (7) (2001)933 - 942.
[4] P.R. Chandra, M.L. Fontenot, J.C. Han, Effect of rib profiles on turbulent channel flow heat transfer, AIAA J. Thermophys. Heat Transf. 12 (1) (1998) 116 - 118.
[5] T.M. Liou, J.J. Hwang, Effect of ridge shapes on turbulent heat transfer and friction in rectangular channel, Int. J. Heat Mass Transf. 36 (4) (1993) 931-940.
[6] Varun, R.P. Saini, S.K. Singal, A review on roughness geometry used in solar air heaters, Sol. Energy 81 (2007) 1340 - 1350.
[7] D. Gupta, S.C. Solanki, J.S. Saini, Thermo-hydraulic performance of solar air heaters with roughened absorber plates, Sol. Energy 61 (1) (1997) 33 - 42.
[8] Bilen, K., Yapici, S., Heat transfer from a surface fitted with rectangular blocks at different orientation angle, Int. J. Heat Mass Transfer, Vol. 38, 2002, pp. 649-655.
[9] S. Eiamsa-ard, P. Promvonge, Numerical study on heat transfer of turbulent channel flow over periodic grooves, Int: Commun. Heat Mass Transf. 35 (7) 844-852, (2008).

[10] Chaube A, Sahoo PK, Solanki SC. Analysis of heat transfer augmentation and flow characteristics due to rib roughness over absorber plate of a solar air heater. Renewable Energy 2006; 31:317–31.
[11] Chaube A, Sahoo PK, Solanki SC. Effect of roughness shape on heat transfer and flow friction characteristics of solar air heater with roughened absorber plate. WIT Transactions on Engineering Sciences 2006; 53:43–51.
[12] Wang C, Guan Z, Zhao X, Wang D. Numerical simulation study on transpired solar air collector. In: Proceedings of the sixth international conference for enhanced building operations, 6–9 November 2006, Shenzhen, China; 2006.
[13] Varol Y, Oztop HF. A comparative numerical study on natural convection in inclined wavy and flat-plate solar collectors. Building and Environment 2008; 43:1535–44.
[14] Kumar S, Saini RP. CFD based performance analysis of a solar air heater duct provided with artificial roughness. Renewable Energy 2009; 34:1285–91.
[15] Karmare SV, Tikekar AN. Analysis of fluid flow and heat transfer in a rib grit roughened surface solar air heater using CFD. Solar Energy 2010; 84:409–17.

